Research papers

Dissolved inorganic carbon export from rivers of Great Britain: Spatial distribution and potential catchment-scale controls

Andrew M. Tye [a,*], Jennifer L. Williamson [b], Helen P. Jarvie [c,d], Nancy B. Dise [l],
Dan J. Lapworth [e], Don Monteith [f], Richard Sanders [g,1], Daniel J. Mayor [g], Michael J. Bowes [d],
Michael Bowes [a], Annette Burden [b], Nathan Callaghan [b], Gareth Farr [h], Stacey L. Felgate [m],
Stuart Gibb [i], Pete J. Gilbert [i], Geoff Hargreaves [j], Patrick Keenan [f], Vassilis Kitidis [k],
Monika D. Jürgens [d], Adrian Martin [g], Ian Mounteney [a], Philip D. Nightingale [k],
M. Gloria Pereira [f], Justyna Olszewska [l], Amy Pickard [l], Andrew P. Rees [k], Bryan Spears [l],
Mark Stinchcombe [g], Debbie White [e], Peter Williams [e], Fred Worrall [n], Chris D. Evans [b]

[a] British Geological Survey, Keyworth, Nottingham, NG12 5GG, UK
[b] UK Centre for Ecology & Hydrology, Environment Centre Wales, Deiniol Road, Bangor, Gwynedd LL57 2UW, UK
[c] Water Institute and Department of Geography and Environmental Management, University of Waterloo, Canada
[d] UK Centre for Ecology & Hydrology, Benson Lane, Wallingford, OX10 8BB, UK
[e] British Geological Survey, Benson Lane, Wallingford OX10 8BB, UK
[f] UK Centre for Ecology & Hydrology, Lancaster Environment Centre, Library Avenue, Bailrigg, Lancaster LA1 4AP, UK
[g] National Oceanography Centre, European Way, Southampton, SO14 3ZH, UK
[h] British Geological Survey, Cardiff University, Main Building, Park Place, Cardiff CF10 3AT, UK
[i] University of the Highlands and Islands, Environmental Research Institute, Castle Street, Thurso KW14 7JD, UK
[j] National Oceanography Centre, Joseph Proudman Building, 6 Brownlow Street, Liverpool L3 5DA, UK
[k] Plymouth Marine Laboratory, Prospect Place, The Hoe, Plymouth PL1 3DHm, UK
[l] UK Centre for Ecology & Hydrology Edinburgh, Bush Estate, Penicuik, Midlothian EH26 0QB, UK
[m] Analytical Chemistry, Department of Chemistry – BMC, Uppsala University, Uppsala, UK
[n] Dept of Earth Sciences, University of Durham, Science Laboratories, South Road, Durham DH1 3LE, UK

ARTICLE INFO

ABSTRACT

Dissolved inorganic carbon (DIC) fluxes from the land to ocean have been quantified for many rivers globally. However, CO_2 fluxes to the atmosphere from inland waters are quantitatively significant components of the global carbon cycle that are currently poorly constrained. Understanding, the relative contributions of natural and human-impacted processes on the DIC cycle within catchments may provide a basis for developing improved management strategies to mitigate free CO_2 concentrations in rivers and subsequent evasion to the atmosphere. Here, a large, internally consistent dataset collected from 41 catchments across Great Britain (GB), accounting for ~36% of land area (~83,997 km²) and representative of national land cover, was used to investigate catchment controls on riverine dissolved inorganic carbon (DIC), bicarbonate (HCO_3^-) and free CO_2 concentrations, fluxes to the coastal sea and annual yields per unit area of catchment. Estimated DIC flux to sea for the survey catchments was 647 kt DIC yr^{-1} which represented 69% of the total dissolved carbon flux from these catchments. Generally, those catchments with large proportions of carbonate and sedimentary sandstone were found to deliver greater DIC and HCO_3^- to the ocean. The calculated mean free CO_2 yield for survey catchments (i.e. potential CO_2 emission to the atmosphere) was 0.56 t C km^{-2} yr^{-1}. Regression models demonstrated that whilst river DIC (R^2 = 0.77) and HCO_3^- (R^2 = 0.77) concentrations are largely explained by the geology of the landmass, along with a negative correlation to annual precipitation, free CO_2 concentrations were strongly linked to catchment macronutrient status. Overall, DIC dominates dissolved C inputs to coastal waters, meaning that estuarine carbon dynamics are sensitive to underlying geology and therefore are likely to be reasonably constant. In contrast, potential losses of carbon to the atmosphere via dissolved CO_2, which likely constitute a significant fraction of

* Corresponding author.
  E-mail address: atye@bgs.ac.uk (A.M. Tye).
[1] Present address: NORCE Norwegian Research Centre, Janhnebakken 5, 5007 Bergen, Norway.

net terrestrial ecosystem production and hence the national carbon budget, may be amenable to greater direct management via altering patterns of land use.

1. Introduction

The transport of dissolved inorganic carbon (DIC) via streams and rivers to estuaries is a significant part of the global C cycle, linking terrestrial, oceanic and atmospheric environments (Meybeck, 1993; Ludwig et al., 1998; Dupré et al., 2003; Aufdenkampe et al., 2011; Ciais et al., 2014). The importance of the DIC cycle over geological periods occurs via the weathering of Ca or Mg silicate rocks, which consumes CO_2 and produces alkalinity (Berner, 1998; Suchet et al., 2003). However, much current interest concerns freshwater and estuarine environments super-saturated with CO_2 that act as a source of greenhouse gases (Rawlins et al., 2014; Hunt et al., 2014; Kitidis et al., 2019; Regnier et al., 2022). A recent estimate indicated that inland waters receive ~1.7 Pg C yr^{-1} of terrestrial carbon transported from soils (Ciais et al., 2014). Of this ~0.2 Pg is buried in aquatic sediments and ~ 0.7 Pg is returned to the atmosphere via gas exchange. The remaining ~0.8 Pg is transported to the oceans as dissolved inorganic and organic carbon and particulate organic carbon.

DIC equilibrates into multiple forms in natural waters (bicarbonate (HCO_3^-), carbonate (CO_3^{2-}) and carbonic acid ($H_2CO_3^*$) and dissolved free CO_2), the concentrations of which vary temporally and spatially in streams and rivers, and with pH and water temperature being key controls on speciation (Jarvie et al., 2017). Major natural influences on concentrations and fluxes of DIC include catchment lithology and mineralogy, mineral weathering rates, altitude, and climate (Chaplot and Mutema, 2021; Kindler et al., 2011; Suchet et al., 2003). Catchment lithology is a major control, with carbonate-dominated catchments typically providing the highest HCO_3^- and CO_3^{2-} concentrations. In Great Britain (GB) this is demonstrated where DIC in carbonate rock-dominated catchments typically exceeds 40 mg L^{-1} whilst in catchments where there are few or no carbonate-bearing rocks, concentrations are typically <10 mg L^{-1} (Jarvie et al., 2017). Altitude and climate also strongly influence catchment DIC flux and speciation, as they influence temperature and precipitation which act as controls on catchment respiration (soil and vegetation), hydrology and the transport of DIC produced from weathering reactions (Drake et al., 2020). Soil-derived CO_2 is reported to account for ~67% of DIC in the world's rivers (Amiotte-Suchet et al., 1999).

The 'natural' catchment processes that integrate to produce riverine DIC fluxes operate over a variety of timescales. Raymond and Hamilton (2018) suggest that DIC fluxes are based on the availability and reactivity of minerals for weathering (supply limitation), the transport of solutes (transport limitation) and volume and residence time of water passing through the system (reaction limitation). On top of these 'natural' DIC producing processes, anthropogenic activities such as those associated with climate warming, acid precipitation, mining and construction have been identified as perturbing riverine DIC fluxes (Drake et al., 2020; Neal et al., 2000; Raymond and Hamilton, 2018; Ren et al., 2015). Increasingly, the impacts of agriculture (Borges et al., 2018; Raymond and Hamilton, 2018) and urbanisation (Jarvie et al., 1997, 2004; Baker et al., 2008; Marescaux et al., 2018; Wang et al., 2017) within catchments are recognised as contributing to changing river DIC flux. Much of this derives from increases in catchment macro-nutrient status, with much research focusing on the increase and evasion potential of greenhouse gases (Billett and Harvey, 2013; Marescaux et al., 2018).

It is evident that human impacts can change the DIC cycle. However, changes to the DIC cycle are unlikely to be in isolation from other biogeochemical cycles. Greater understanding of the interactions of these cycles is needed, for example, how perturbations to coupled P, N and C cycles impact degassing of CO_2 from rivers. Management solutions

aimed at reducing nutrient inputs to rivers (e.g. improved nutrient management, implementation of agricultural conservation practices and, improvements in sewage treatment) are being increasingly used, whilst newer ideas such as re-balancing macro-nutrient stoichiometry within catchments are being developed (Stutter et al., 2018; Graeber et al., 2021). In addition, technologies being suggested to mitigate rising CO_2 levels may also influence exports of DIC in future; for example, the application of ground basalt to soils appears to be a technology gaining support as a form of greenhouse gas removal, as a means of accelerating chemical weathering and subsequent drawdown of CO_2 (Beerling et al., 2020; Kelland et al., 2020).

Improved understanding and quantification of the responses of the DIC cycle to land-use change and management are therefore required for modelling of C fluxes from land to oceans (and atmosphere). Key uncertainties include (i) understanding the extent to which land use impacts the underlying geological, geomorphological, weathering and catchment processes, (ii) identifying the main drivers of CO_2 flux to the atmosphere and DIC flux to the sea and (iii) gas transfer velocities, which are still poorly constrained. These uncertainties are demonstrated in reports where global CO_2 evasion from inland waters has been estimated as being up to ~4 Gt C yr^{-1} (Ciais et al., 2014; Raymond et al., 2013; Drake et al., 2017). This paper addresses the first two of these uncertainties through a year-long sampling survey in which 41 rivers were sampled, with catchments covering 36% of the GB landmass. The results focus on the spatial concentrations (mg L^{-1}), fluxes (kt yr^{-1}) and yields (T Km^{-2} yr^{-1}) of DIC, HCO_3^- as the dominant aqueous species, and free CO_2. The work explores how current land-use and human activities may impact the 'natural' background gradient controls on DIC concentrations, flux and yield.

2. Materials and methods

2.1. Survey outline

Great Britain (GB: Scotland, Wales and England) has a temperate climate. It is considerably smaller in size than some of the major basins including the Congo (Drake et al., 2020) and the Mississippi (Raymond and Hamilton, 2018) where previous experimental work on DIC has been undertaken, and it has a number of geographical gradients (Jarvie et al., 1997, 2017) that have been recognised as fundamental controls on riverine DIC flux and yield. The survey sampled rivers ($n = 41$) that drain ~36% of GB (defined as being both the mainland and islands; 233,327 km^2) (Fig. 1). The catchments selected are representative of the land cover of GB as a whole (SI 1). The most widespread land cover type sampled, according to the UKCEH Land Cover Map (LCM) 2015, was improved grassland (28% for GB cf. 29% for the catchments sampled) followed by arable land (24% of both GB and catchments sampled) and then acid grassland (9% for GB and cf. 11% for the catchments). Sampling sites were located close to (but always above) the tidal limits, the defined boundary for terrestrial to marine C export in this work (Williamson et al., 2021), and where either the National River Flow Archive (NRFA) (https://nrfa.ceh.ac.uk/) or the UK Harmonised Monitoring Scheme (HMS) sites (https://data.gov.uk/dataset/bda4e065-41e5-4b78-b405-41c1d3606225/historic-uk-water-quality-sampling-harmonised-monitoring-scheme-summary-data) provide long-term water export and quality monitoring.

The GB area incorporates gradients in geology, soils, precipitation, temperature and land use intensity (SI: 2–5). GB has north-south and west-east trends in both geology and altitude. Typically, catchments with large proportions of carbonate-based sedimentary rock are situated in southern and eastern GB, whilst catchments predominantly
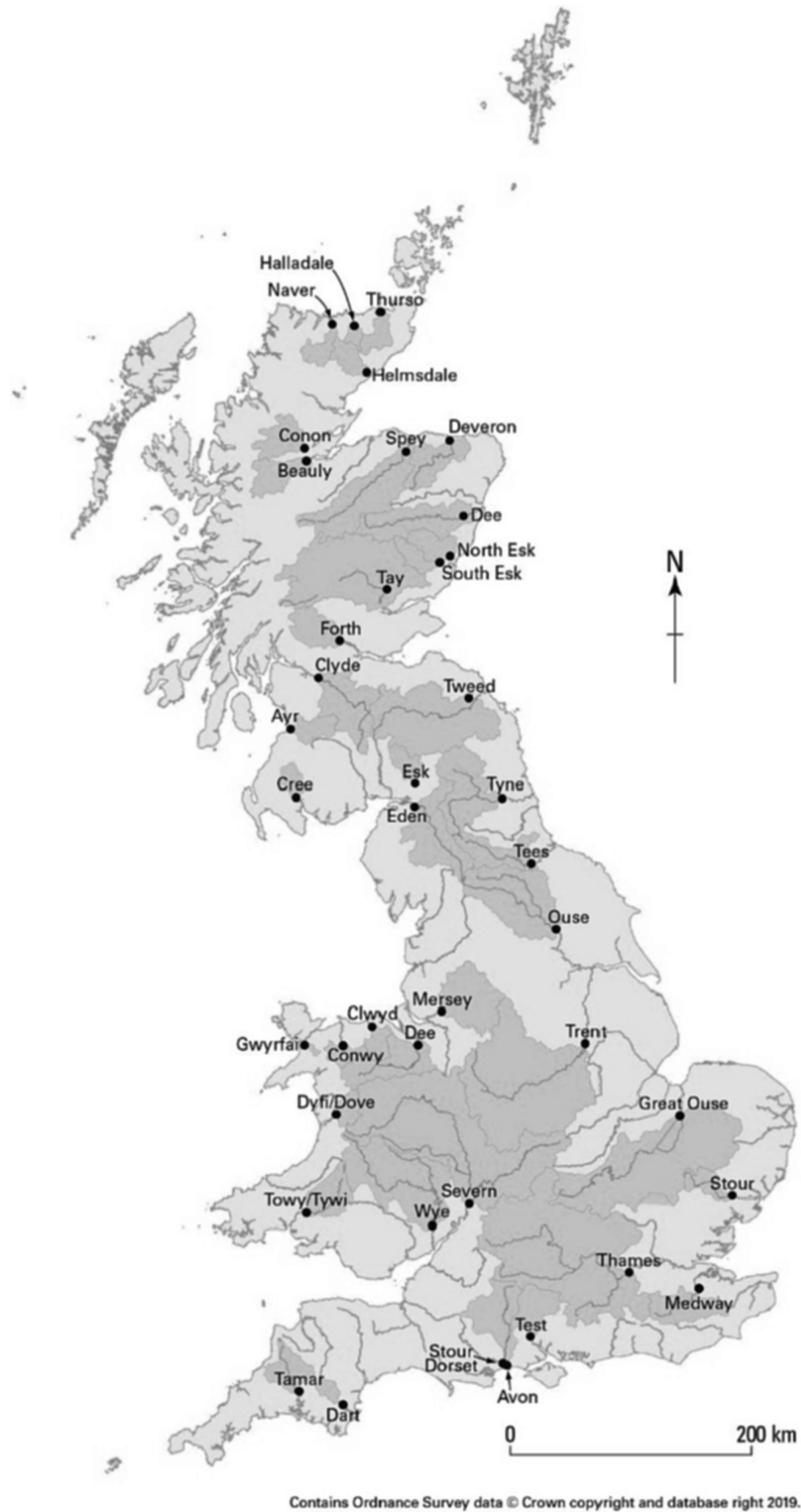
Fig. 1. Sampling sites for catchments across Great Britain.

comprised of weathering-resistant silicate rocks are found to the north and west. Altitude influences both precipitation and temperature, and follows a similar pattern with the highest-altitude catchments generally in the north and west. With the prevailing wind coming from the southwest, and higher land elevation predominantly in the west, precipitation follows a gradient from west to east. Land cover reflects the intensity of soils, agriculture and urbanisation. Soils generally track geology and are more acidic and organic rich in the north and west of the country, whilst more alkaline mineral soils are found in the south and east of the country. In the south eastern quarter of GB, the topography and climate are more conducive to intensive agriculture, with upland agriculture and peatland dominating landscapes in the north and west.

2.2. Sampling and collection methods

A major aim of the survey was to ensure a consistency of approach, equipment and methodologies for calculating riverine carbon fluxes (Tye et al., 2020). Samples for specific determinants were analysed by one laboratory for the duration of the project. Rivers were sampled monthly from January 2017 to December 2017. Samples were collected during the third week of each month, to minimise within-month temporal variation between catchments, especially variation associated with antecedent weather. Water samples were taken from the centre of the river or from fast flowing water away from the river bank. Water temperature and conductivity were measured and recorded immediately after sample collection. Samples for pH and alkalinity were collected unfiltered into 250 ml HDPE bottles to overflowing and sealed to avoid potential changes in speciation due to gaseous exchange. Samples were distributed after collection to their respective analytical centres under cool conditions (ice bags and ice packs) using overnight couriers.

2.3. Laboratory analysis

A Skalar SP10 robotic auto sampler connected to an inoLab 730 pH meter with a SenTix 60 probe was used to measure pH. Alkalinity was determined by titration using a Metrohm 814 sample processor and Metrohm 888 Titrando diluter which undertakes analyses using automatically predefined methods. Analyses of total dissolved carbon (TDC) and non-purgeable organic carbon (NPOC) were used to calculate dissolved inorganic carbon (DIC) concentrations. A Shimadzu TOC-L analyser was used to measure NPOC in filtered and acidified (1 M HCl) samples). The method to determine TDC was the same as above, without the acidification and purge step to remove inorganic carbon (Williamson et al., 2021). Limits of detection for NPOC and TDC were 0.6 mg C L^{-1}. See SI:9 for sampling and analysis details of Total Nitrogen (TN) and Total Phosphorus (TP).

2.4. Use of the THINCARB model for calculating dissolved inorganic carbon speciation and excess

2.4.1. Partial pressure of carbon dioxide from pH and alkalinity

The THINCARB model (THermodynamic modelling of INorganic CARBon; Jarvie et al., 2017) uses pH, temperature and Gran Alkalinity (Alk$_{Gran}$) measurements to calculate dissolved inorganic carbon concentration and speciation from excess partial pressure of CO_2 (EpCO$_2$; x atmospheric pressure) in the water sample compared to the dissolved CO_2 concentration found in pure water in equilibrium with the atmosphere at the same temperature and pressure. THINCARB is open access and is described in detail in Jarvie et al. (2017), an outline is provided in SI:6. THINCARB works effectively across the range pH > 6 and < 10. In our dataset ($n = 521$), 6 samples (1.15%) were found to be below pH 6 with the highest pH value being 9.29. The total sum of dissolved inorganic carbon (DIC$_{Total}$) represents the sum of C concentrations in all the inorganic C species:

$$DIC_{Total}\left(mg\ L^{-1}\right) = C_{C\ in\ HCO_3^-} + C_{C\ in\ H_2CO_3^*} + C_{C\ in\ CO_3^{2-}} \tag{1}$$

After speciation calculations, the percentage contribution of each species in DIC$_{Total}$ was applied to the measured (by difference), inorganic carbon concentration (DIC$_{Measured}$), and used in the interpretation of survey results. Thus, the term 'DIC' used in this paper to describe results corresponds to DIC$_{Measured}$, which was determined as:

$$
\begin{aligned}
DIC_{Measured}\left(mg\ L^{-1}\right) &= Total\ Dissolved\ Carbon\ (TDC)\\
&\quad - Non\ Purgeable\ Organic\ Carbon\ (NPOC)
\end{aligned}
\tag{2}
$$

Values of EpCO$_2$ were used to estimate 'free CO$_2$-C' concentrations in the water samples (described as free CO_2 in text). The CO_2 concentration equals pCO$_2$ times the solubility of CO_2 corrected using water temperature (Henry's law constant at a given temperature and salinity). Thus:

$$Free\ CO_2C = K_h\ x\ pCO_{2,w} - K_h\ x\ pCO_{2,a} \tag{3}$$

Where K$_h$ represents Henry's law constant for freshwater and corrected for water temperature, pCO$_{2,w}$ and pCO$_{2,a}$ are the pCO$_2$ in the surface water and the pCO$_2$ in equilibrium with the overlying air, respectively (Wang et al., 2017).

2.5. Ancillary data

Ancillary data used in the statistical and modelling analysis were the same as used in Williamson et al. (2021) which describes the DOC results from this survey, enabling consistent comparison between the DIC and DOC results. Mean catchment altitude and average annual precipitation (as Standard period Average Annual Rainfall (SAAR)) were included in the modelling data set, both being likely key gradients for controlling DIC across GB (see SI:3 and SI:4). Catchment area and land cover characteristics (14 broad habitats) were obtained from the 2015 UKCEH Land Cover Map 2015 (Rowland et al., 2017a, 2017b) and are shown in SI:5. The different grassland types were not aggregated as they typically represent soils with different pH values (e.g. acid or calcareous grassland) or where pH may be manipulated using agricultural lime (e.g. improved grassland), thus influencing river DIC concentrations (see SI:5).

Additional variables included the percentage of carbonate and sedimentary sandstone in survey catchments (see SI:2). These were obtained by combining UK catchment and sub-catchment maps with the BGS 50 k soil parent material model and using the European Soil Bureau bedrock classification. Catchment areas of basalt and shale, known to be important in CO_2 drawdown via silicate weathering, were obtained in a similar manner. However, the contributions from these rocks to catchment geology was minimal. Estimates of catchment population were made by summing the proportion of population for each local authority area that intersected the catchment.

Mean daily gauged river flows were obtained from the national agencies for England, Scotland and Wales (Environment Agency (EA), Scottish Environmental Protection Agency (SEPA) and Natural Resources Wales (NRW), respectively. At most sites, water sampling and flow gauging were located within a few hundred metres of each other. Flows at the gauging station were assumed to be indicative of those at the water sampling site. Upstream gauging data were used to estimate flows for four rivers (Eden, Mersey and Welsh Dee), where co-located flow data were not available during 2017. Past annual discharge data were calculated for each comparison gauging station to ensure that total annual discharge was estimated to within 10% of observations, with a correction made to the annual discharge calculation for 2017 if differences between upstream and downstream gauging stations were >10%. The relationship between upstream and downstream daily flows during 2015, the most recent year with comparable data, was calculated using regression analysis, and daily flows for the sampling site for 2017 were estimated from the regression equation (Williamson et al., 2021). Daily flows for the Conon were used to represent those in the nearby Beauly assuming the same mean areal runoff for both catchments, since they are similar in area and topography. Daily flow data for 2017 were

unavailable for the Dyfi, whilst only half a year's data was collected for the Dorset Stour, so these two rivers were excluded from calculations of DIC flux and yield. Catchment mean elevation (m) and area along with hydrogeology including Base Flow Index were obtained from the UK National River Flow Archive (NRFA) (http://nrfa.ceh.ac.uk).

2.6. Data treatment

All statistical analysis was undertaken using the R statistical package v3.5.1 (R Core Team, 2018). Stepwise regression analysis was undertaken using the 'MASS' and 'leaps' packages to identify the explanatory land-use and hydrogeological variables that best predicted the concentrations of DIC species. A complete list of variables used in the regression analysis can be found in SI:7. Prior to running regression models, correlation matrices were used to eliminate variables where co-linearity was exhibited. The model selected was the one which reported the lowest Bayesian Information Criteria (BIC) value. Tests for skewness were undertaken on the dependent variables and were Log$_{10}$ transformed if skewness was < -1 or > 1. EpCO$_2$ values were converted into concentrations of free CO$_2$ prior to models being parameterised. For river free CO$_2$ concentrations, initial modelling was carried out using the above dataset and a second dataset of river mean macronutrient concentrations collated from the survey data.

DIC fluxes were calculated using "method 5" of Littlewood et al. (1998) to be consistent with data analysis for the DOC component of the study undertaken in Williamson et al. (2021). Some underestimation may occur using such methods as compared to using high resolution data (Worrall et al., 2013). 'Method 5' is detailed in Eq. (4), whereby k specifies a conversion factor for the length of sampling, C$_i$ refers to the DOC concentration at sampling time i, Q$_i$ refers to flow at sampling time i, Q$_T$ refers to the mean flow over the whole sampling period, and n is the number of samples taken.

$$DIC\ flux = k\ \frac{\sum_{i=1}^{n} [C_i Q_i]}{\sum_{i=1}^{n} Q_i} Q_T \quad (4)$$

Stepwise regression analysis was again undertaken on the annual river flux estimates to identify the explanatory variables that most likely explained the annual flux across GB.

3. Results

3.1. Initial dataset

The relationship between the THINCARB modelled DIC data and the measured (by subtraction) alkalinity results (SI:8) was significant (y = 0.9525×-0.4572; R^2 = 0.99, n = 518), giving confidence to the interpretation of the modelling results. Some over-prediction of DIC occurred when DOC concentrations were high, due to the greater role for organic C buffers such as organic acids (Jarvie et al., 2017). Fig. 2 describes the range of concentrations of DIC species for the entire survey (mg C L^{-1}) for DIC, HCO$_3^-$, CO$_3^{2-}$ and H$_2$CO$_3$*. As expected, for the range of pH values recorded, HCO$_3^-$ dominated DIC, accounting for >80% of DIC in river waters with pH >7 and 40–80% of DIC in rivers with pH <7. A median HCO$_3^-$ concentration of ~10 mg C L^{-1} was found. The highest values (>95th percentile) for HCO$_3^-$ exceeded 57 mg C L^{-1} and were associated with two rivers (Stour and the Great Ouse in Eastern England) with high proportions of chalk geology (44 and 95% respectively) within their catchments. These catchments also received the two lowest annual average precipitation rates (580 and 587 mm yr-1 respectively). The contribution of CO$_3^{2-}$ was low across the sites, with a median value <1 mg C L^{-1}, whilst H$_2$CO$_3$* concentrations were generally <2 mg C L^{-1}. Most samples had EpCO$_2$ values >1, representing oversaturation with respect to atmospheric CO$_2$ partial pressure, and suggesting potential efflux of CO$_2$ from rivers to the atmosphere. Only 2% of EpCO$_2$ results had values <1, indicating under-saturation with respect to atmospheric pressure, suggesting potential influx of CO$_2$ to rivers from the atmosphere. The 95th percentile value of EpCO$_2$ results was 9.6 × atmospheric partial pressure and the highest estimated value was 21.3 × atmospheric partial pressure.

3.2. Spatial patterns of DIC$_{Measured}$, HCO$_3^-$ and free CO$_2$ concentrations across GB

The highest flow-weighted mean concentrations of DIC were found in England and southern Scotland (Fig. 3a) and the lowest concentrations were found in the west of England, Wales and north-eastern Scotland. This pattern demonstrates the role of the catchment bedrock geology, particularly those with high proportions of carbonate rocks, on DIC concentrations. Flow-weighted mean HCO$_3^-$ concentrations showed a similar pattern, as HCO$_3^-$ generally makes up the greatest proportion of DIC in these catchments (Fig. 3b). The spatial pattern of concentrations of free CO$_2$ (mg C L^{-1}) (Fig. 3c) showed the highest concentrations in the peat-dominated Halladale catchment, and the River Mersey in
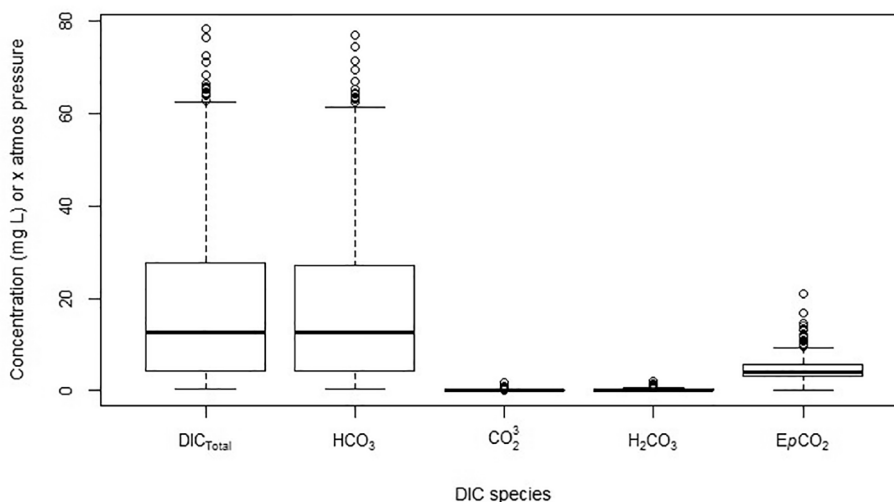

Fig. 2. Boxplots showing the ranges of DIC$_{Total}$, HCO$_3^-$, CO$_3^{2-}$, H$_2$CO$_3$ (mg L^{-1}) and EpCO$_2$ (x atmospheric pressure) for the 41 rivers sampled on a monthly basis.
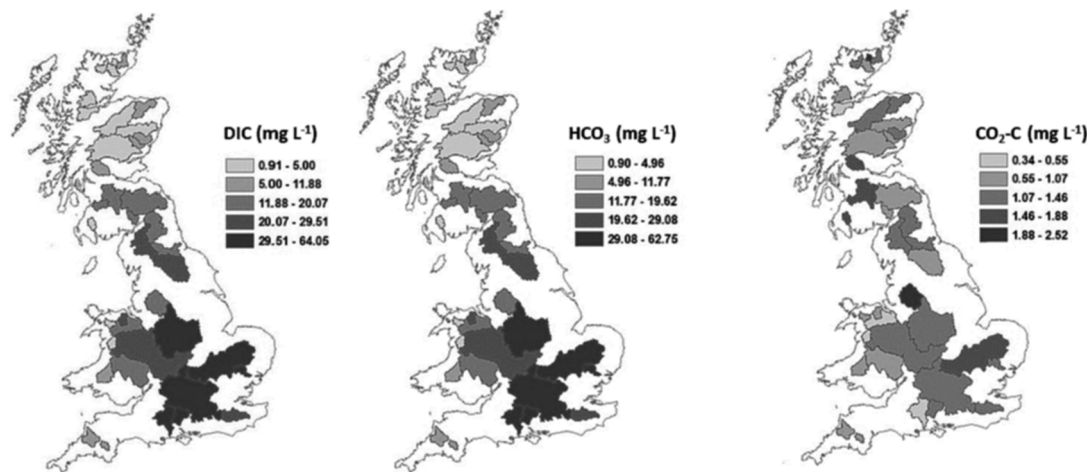
Fig. 3. Spatial patterns of annual (a) Mean Flow Weighted (MFW) mean DIC (mg L^{-1}), (b) MFW mean HCO_3^- and (c) MFW mean CO_2-C concentrations across the UK for monthly river samples taken during 2017. Contains OS data © Crown copyright and database right 2022.

Northwest England. Catchments in the west of Scotland, along with the large lowland agricultural catchments of southern GB, also demonstrated relatively high concentrations of free CO_2.

3.3. Modelling concentrations of DIC species using catchment land cover and catchment characteristics

The best fit model to predict DIC had an R^2 of 0.77 (Table 1). In this model DIC was positively correlated with the percentages of carbonate rocks and sedimentary sandstone within the catchment and negatively correlated with average annual precipitation and heather grassland area. Whilst most GB catchments possess a small area of heather grassland, it is the catchments of northern Britain that generally have greater areas. The inclusion of heather grassland increased the R^2 to 0.72 from 0.77. The best model for HCO_3^- ($R^2 = 0.77$) included the catchment percentages of carbonate and sedimentary sandstone rocks and the base flow index (BFI) (positive coefficients), and the percentage of heather grassland and average annual precipitation (negative coefficients) (Table 2). In a similar manner to the DIC model, the inclusion of the land cover variable heather grassland increased the model R^2 from 0.69 to 0.77.

The initial regression model for free CO_2 concentrations used only catchment characteristics in the pool of potential explanatory variables. It had an R^2 value of 0.50 and included altitude (negative coefficient) and neutral grassland (positive coefficient). A second model based on the river macro-nutrient concentrations (TN, TP and DOC) produced an R^2 of 0.72 (Table 3). No improvement was found in model prediction using PO_4-P and NO_3-N, as they were highly correlated with TP and TN ($r = 0.99$ and $r = 0.98$) respectively.

Table 1
Output from stepwise regression analysis to predict mean Log_{10} DIC_{Total}-C concentrations (mg L^{-1}).

	Estimate	Std. Error	t value	Significance
(Intercept)	1.493e+00	1.292e-01	11.556	1.69e-13 ***
Carbonate rocks	6.853e-03	1.647e-03	4.160	0.000196 ***
Sandstone	2.461e-02	8.231e-03	2.990	0.005083 **
Annual precipitation	-5.007e-04	9.244e-05	−5.417	4.54e-06 ***
Heather grassland	−1.229e-05	5.523e-06	−2.226	0.032578 *

Signif. codes:
0 '***' 0.001 '**' 0.01 '*' 0.05 '.' 0.1 ' ' 1.
Residual standard error: 0.2342 on 35 degrees of freedom.
Multiple R-squared: 0.7747, Adjusted R-squared: 0.749.
F-statistic: 30.09 on 4 and 35 DF.
p-value: 6.839e-11.

Table 2
Output from stepwise regression analysis to predict mean Log_{10} HCO_3^- concentrations (mg L^{-1}).

	Estimate	Std. Error	t value	Significance
Intercept	9.331e-01	2.617e-01	3.566	0.00110 **
Carbonate rocks	5.631e-03	2.269e-03	2.481	0.01819 *
Annual precipitation	−5.284e-04	1.155e-04	−4.577	6.03e-05 ***
BFI	9.974e-01	4.140e-01	2.409	0.02156 *
Heather grassland	−1.875e-05	7.068e-06	−2.653	0.01205 *
Sandstone	2.889e-02	1.005e-02	2.874	0.00695 **

Signif. codes:
0 '***' 0.001 '**' 0.01 '*' 0.05 '.' 0.1 ' ' 1.
Residual standard error: 0.286 on 34 degrees of freedom.
Multiple R-squared: 0.7749, Adjusted R-squared: 0.7418.
F-statistic: 23.41 on 5 and 34 DF.
p-value: 4.005e-10.

Table 3
Output from stepwise regression analysis to predict mean $Log_{10}CO_2$-C concentrations (mg L^{-1}) across 40 rivers in Great Britain.

	Estimate	Std. Error	t value	Significance
Intercept	0.1193	0.0758	1.574	0.123
DOC	0.0331	0.0087	3.775	***
Total N	0.0359	0.0148	2.423	*
Total P	0.7949	0.2269	3.503	**

Signif. codes: 0 '***' 0.001 '**' 0.01 '*' 0.05 '.' 0.1 ' ' 1.
Residual standard error: 0.1519 on 37 degrees of freedom.
Multiple R-squared: 0.723, Adjusted R-squared: 0.7005.
F-statistic: 32.19 on 3 and 37 DF, p-value: 2.064e-10.

3.4. Spatial distribution of DIC, HCO_3^- and free CO_2 flux (kt yr^{-1}) from rivers to the coastal sea

Fig. 4 shows the spatial distribution of DIC, HCO_3^- and free CO_2 flux from rivers across Great Britain. The total flux (t yr^{-1}) of these species largely reflected catchment size (which scales with total water discharge). A total combined flux of DIC of 647 kt DIC yr^{-1} was calculated from the sampled rivers. As HCO_3^- is the predominant species in the samples, the annual flux was 636 kt C yr^{-1} and for free CO_2-C it was 47.6 Kt C yr^{-1}.

3.5. Spatial distribution of DIC, HCO_3^- and free CO_2 yield (t km^{-2} yr^{-1})

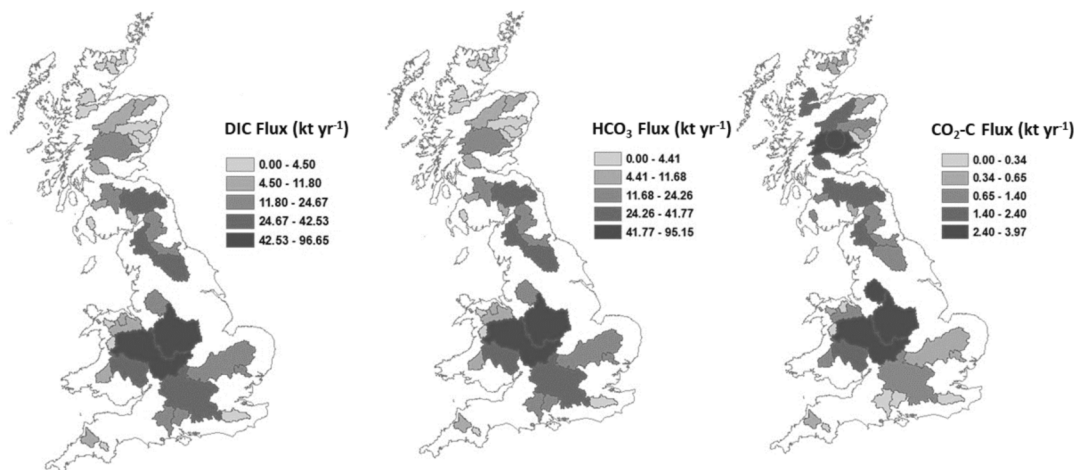Catchment estimates of DIC fluxes were converted to estimates of

Fig. 4. Spatial patterns of annual flux (kt yr^{-1}) of (a) DIC, (b) HCO$_3^-$ and (c) CO$_2$-C concentrations across the UK for monthly river samples taken during 2017. Contains OS data © Crown copyright and database right 2022.

yield (t C km^{-2} yr^{-1}), with the range varying between 1.3 and 33.3 t C km^{-2} yr^{-1} for the rivers Helmsdale and Stour, respectively (Fig. 5a). Other than the Stour catchment, which is chalk dominated, higher DIC$_{Total}$ yield was associated with catchments on the western side of GB, where there is generally greater precipitation resulting in higher drainage. A similar pattern was found for HCO$_3^-$ (Fig. 5b). For free CO$_2$ yield (t C km^{-2} yr^{-1}), the smaller, upland catchments of Scotland, had the highest yields (Fig. 5c). The larger agricultural catchments and lowland catchments of southern England had lower yields.

3.6. Modelling yield of DIC species using catchment landcover characteristics

Using stepwise regression, the significant land cover and catchment variables for predicting DIC yield were % carbonate rocks and acid grassland (positive coefficients), and peat (negative coefficient). The model had an R^2 of 0.37 (Table 4). For HCO$_3^-$ the coefficients were similar to those for DIC (Table 5). The stepwise regression for free CO$_2$ yield (Table 6) had an R^2 = 0.67, and the coefficients selected were negative for both the area of arable agriculture in catchments and BFI.

4. Discussion

4.1. DIC budgets and their contribution to terrestrial C loss

A combined total DOC and DIC flux of 938 kt was estimated in the 39 river systems with flow data sampled in 2017. The 2017 flux of DIC to the estuaries, 647 kt DIC yr^{-1}, is more than double the estimated DOC export of 290 kt for the same rivers and time period as reported by Williamson et al. (2021). The DIC contribution is therefore ~69% of
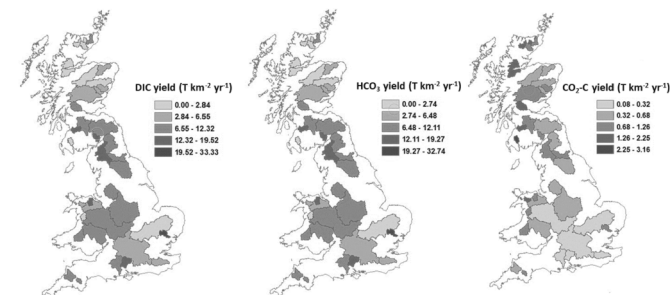
Table 4
Output from stepwise regression analysis to predict Log$_{10}$ DIC$_{Total}$ yield (t km^2 yr^{-1}) across 39 rivers in Great Britain.

	Estimate	Std. Error	t value	Significance
Intercept	7.206e-01	7.620e-02	9.457	3.58e-11 ***
Peat	−7.769e-06	2.519e-06	−3.084	0.00397 **
Acid grassland	4.888e-06	1.693e-06	2.888	0.00661 **
Carbonate rocks	6.880e-03	1.945e-03	3.538	0.00116 **

Signif. codes:
0 '***' 0.001 '**' 0.01 '*' 0.05 '.' 0.1 ' ' 1.
Residual standard error: 0.2982 on 35 degrees of freedom.
Multiple R-squared: 0.3698, Adjusted R-squared: 0.3158.
F-statistic: 6.845 on 3 and 35 DF,
p-value: 0.0009486.

Table 5
Output from stepwise regression analysis to predict Log$_{10}$ HCO$_3^-$ yield (t km^2 yr^{-1}) across 39 rivers in Great Britain.

	Estimate	Std. Error	t value	Significance
Intercept	7.139e-01	7.667e-02	9.311	5.31e-11 ***
Peat	−7.764e-06	2.535e-06	−3.063	0.00420 **
Acid grassland	4.915e-06	1.703e-06	2.886	0.00664 **
Carbonate rocks	6.803e-03	1.957e-03	3.476	0.00138 **

Signif. codes:
0 '***' 0.001 '**' 0.01 '*' 0.05 '.' 0.1 ' ' 1.
Residual standard error: 0.3 on 35 degrees of freedom.
Multiple R-squared: 0.3646, Adjusted R-squared: 0.3102.
F-statistic: 6.696 on 3 and 35 DF.
p-value: 0.001086.

Table 6
Output from stepwise regression analysis to predict Log$_{10}$ CO$_2$-C yield (t km^2 yr^{-1}) across 39 rivers in Great Britain.

	Estimate	Std. Error	t value	Significance
Intercept	5.060e-01	1.281e-01	3.952	***
Arable	−1.822e-06	3.257e-07	−5.595	***
BFI	−1.112e+00	2.558e-01	−4.345	***

Significance codes: 0 '***' 0.001 '**' 0.01 '*' 0.05 '.' 0.1 ' ' 1.
Residual standard error: 0.2022 on 36 degrees of freedom.
Multiple R-squared: 0.6731, Adjusted R-squared: 0.6549.
F-statistic: 37.06 on 2 and 36 DF, p-value: 1.818e-09.

Fig. 5. Spatial patterns of annual yield (T km^{-2} yr^{-1}) of (a) DIC, (b) HCO$_3^-$ and (c) CO$_2$-C concentrations across the UK for monthly river samples taken during 2017. Contains OS data © Crown copyright and database right 2022.

total GB aquatic carbon export. Similarly, DIC accounted for 63% of dissolved carbon export in a global analysis of river dissolved carbon flux (Li et al., 2017). A recent study of 39 years of Harmonised Monitoring Scheme data suggested that DIC accounted for an average of 80% of the total TDC flux from the UK's 7 largest rivers (Severn, Thames, Trent, Wye, Great Ouse, Ouse, Tay) (Jarvie et al., 2017). DIC export from the same rivers in our one-year study comprised, on average, 78% of the TDC flux, demonstrating excellent comparability. Thus, our study confirms that DIC makes a dominant contribution to the GB annual land-ocean C budget. For the DOC results in this survey, Williamson et al. (2021) modelled an annual export of DOC from GB of 1150 kt C yr^{-1} which produced an upscaling factor of 3.96 from the survey results to GB scale. This figure was used to obtain a 'first-order' estimate DIC flux for GB of 2560 kt C yr^{-1} for 2017. This estimate is within the range of 2000–3000 kt C yr^{-1} modelled using the LTLS macro-nutrient model for GB (Bell et al., 2021).

The DIC yields (t C km^{-2} yr^{-1}) determined in this survey are of similar magnitude to those reported previously for the long-term HMS monitoring dataset of the UK (Jarvie et al., 2017). Yields from the 246 rivers in the Harmonised Monitoring Scheme (HMS) ranged from 6.8 t C km^{-2} yr^{-1} in the Tay to 17.7 t C km^{-2} yr^{-1} in the Yorkshire Ouse and Trent over the years 1974–2012. DIC yields calculated from the 2017 survey range from 1.2 t C km^{-2} yr^{-1} for the Helmsdale (which wasn't available as part of the HMS dataset in the Jarvie et al. (2017) analysis), to 33.3 t C km^{-2} yr^{-1} for the Stour. The mean DIC values for the two surveys were compared where data ($n = 35$) existed (SI 9). An R^2 of 0.95 was found with a slope of 0.99 between the two sets of data suggesting that concentrations were largely comparable, even though they represent two very different time periods (i.e. 36 years for the HMS monitoring dataset and 1 year in the current study). With respect to the 2017 survey, precipitation was close to the long-term average (https://www.metoffice.gov.uk/about-us/press-office/news/weather-and-climate/2017/weather-review-of-2017), with a UK average of 1106 mm being 95.9% of the long-term average (1981–2010). This comparison suggests the 2017 results are not biased towards an extreme dry or wet year.

4.2. Controls on DIC and HCO_3^- concentrations

DIC and HCO_3^- concentrations were strongly associated with geology and geomorphology (i.e. rock type, altitude and precipitation). The important variables driving the concentration of DIC and HCO_3- are identified in the regression models (Tables 1 & 2). The relationships between these variables and DIC concentrations are demonstrated in plots (SI:10). High concentrations of DIC and HCO_3^- were found in catchments with a large percentage of either carbonate or sedimentary sandstone (e.g. Severn). Sedimentary sandstones contain carbonate cements in their mineral matrices and are a known additional source of HCO_3^- through the weathering of this cement. The graphs in SI:10 show that there are no direct relationships between % of carbonate and sandstone in catchments and the DIC concentrations. Catchments will often contain both of these lithologies, and the form of carbonate rocks may be chalk, limestone or both. The regression models identify the relative contributions of both. Rivers draining silicate rocks (e.g. Spey, Dee Scotland and Tay) produced the lowest concentrations of DIC and HCO_3^- (< 5 mg L^{-1}). A global analysis of the contributions of major rock types to drawdown of CO_2 through weathering reactions identified the importance of carbonate and sedimentary sandstone (Suchet et al., 2003). Basalts are particularly recognised for their ability to draw down CO_2 through Ca and Mg-silicate weathering, whilst the magnitude is less for shales (Suchet et al., 2005). However, none of the monitored catchments had large percentages of shale or basalt geology.

The chalk, limestone and sedimentary sandstone lithologies also contribute to high catchment base flow, identified as positive coefficients in both the DIC and HCO_3^- concentration models (the relationship between Base Flow and DIC concentrations is shown in SI:10). A negative relationship between DIC and HCO_3^- concentrations with

annual precipitation was reported in the models (and shown in SI:10). Altitude was also identified by the regression models and had a strong negative relationship (see SI:10). The influence of altitude and precipitation is linked. Firstly, at the highest mean altitudes, catchments are predominantly comprised of non-carbonate geology. Secondly, as altitude increases, the contribution of soil-derived DIC decreases, as a result of shorter growing seasons, typically thinner soils, and reduced annual mean temperatures that constrain rates of ecosystem respiration and weathering. Altitude and prevailing wind direction also create the precipitation gradient from west to east across GB. The negative coefficients for average annual precipitation in the DIC and HCO_3^- concentration models likely identifies the lowland, drier areas in the south east of the country that also tend to have the highest percentages of carbonate geology within catchments. The inclusion of heather grassland as a land cover variable in both the DIC and HCO_3^- concentration models, where it increased R^2 by small amounts, is likely acting as a proxy for acid peaty soils and accounting for extra variability regarding low DIC and HCO_3^-.

The DIC and HCO_3^- concentration models demonstrate the influence of geology and other associated physical gradients (e.g. altitude, average annual precipitation) on the spatial pattern of their concentrations. Previous studies have suggested some human influences on river DIC concentrations, particularly around land-use change (Raymond et al., 2008), urbanisation (Barnes and Raymond, 2009) or the use of soil liming materials (e.g. Oh and Raymond, 2006; Stets et al., 2014). In this study, it is the large agricultural and urbanised catchments of southern England where greater human impacts on DIC concentrations may be expected. However, indicators of human impact such as catchment population and the area of catchment urbanisation were not identified within the regression analysis.

Whilst the regression models were based on MFW concentrations of DIC and HCO_3^-, seasonal and water flow influences were also examined. These are shown for individual rivers in SI:11 &12. Overall, there was relatively little influence of either season or flow on concentrations of DIC and HCO_3^- (SI: 11 & 12). For those catchments with greater % chalk and sandstone-based catchments (Avon, Great Ouse, Stour, Test, Thames, Trent) there were slightly higher concentrations of DIC in the winter (Jan – Mar).

4.3. Catchment controls on DIC yield

The total flux (t yr^{-1}) of DIC and HCO_3^- from catchments largely reflected catchment size and average annual precipitation which promotes the flushing of the products of silicate weathering and respiration (Öquist et al., 2009). When flux is converted to yield (t km^{-2} yr^{-1}) the effect of precipitation is apparent for much of the country, with only the small chalk-based Stour catchment having a high yield when compared to western GB. Both the DIC and HCO_3^- yield models were parameterised using the variables carbonate rocks (+), peat (−) and acid grassland (+). Whilst the carbonate rock and peat variables describe the end points of catchment geochemistry with respect to DIC concentrations, the acid grassland represents the best descriptor of catchments with high precipitation and soils with pH values <5.5. Thus, a greater proportion of DIC and HCO_3^- may be derived from soil respiration and silicate weathering and flushed from the terrestrial system through high rates of rainfall and runoff. Acid grassland is predominantly found in the wetter western and northern parts of GB (see SI:5) and highlights the influence of precipitation and altitude. In addition, many of the large catchments (e.g. Thames (chalk & limestone), Severn (sandstone), Trent (sandstone and limestone) and Great Ouse (chalk)) have large areas where precipitation effectively recharges major groundwater aquifers, which will result in lower surface runoff to river systems. Thus, whilst the geology may largely control concentrations of DIC and HCO_3^-, the distribution of precipitation is a key variable for yield. The importance of annual average precipitation was also seen in the DOC yield model produced from results of this sampling program (Williamson et al., 2021). For the yield of DOC across GB, a model that explained 90% of the variability

was obtained with only three variables (annual average precipitation, % Peat soils and % Forest).

4.4. Catchment controls on concentrations of free CO_2

Beyond the estimation of DIC flux and yield, particular interest lies in the factors that contribute to the concentration and spatial distribution of free CO_2 in the river waters. This pool is potentially available for atmospheric exchange (Harley et al., 2015). It has been shown that as catchment size increases, the residence time increases and concentrations of free CO_2-C may reflect more in-stream processes rather than catchment processes (particularly groundwater inputs) as stream water will get close to $EpCO_2 = 1$ (Worrall and Lancaster, 2005). Sources of free CO_2 from terrestrial ecosystems include soils and groundwater. It can also be generated within river, particularly through the respiration of terrestrial and autochthonous derived DOC. Results showed that the large southern catchments with a high percentage of carbonate geology generally had relatively high concentrations of dissolved free CO_2 (Fig. 3c), although it may be expected that because of their higher water pH values, a smaller fraction of the DIC would exist as free CO_2. Two catchments in particular had very high free CO_2 concentrations. Firstly, the River Mersey, possibly due to large sewage effluent contributions as previously identified by Jarvie et al. (2017). Secondly, the Halladale (the most northerly catchment) which had high $EpCO_2$ year-round but had a dramatic increase in $EpCO_2$ in September 2017, reaching 20 x atmospheric CO_2. The Halladale catchment drains the large Flow Country blanket bog, and flushing of free CO_2 from catchment respiration is suspected as the likely cause here.

Concentrations of free CO_2 were of similar magnitude to those found by Rawlins et al. (2014) who estimated median free CO_2 concentrations in May and November across England and Wales as 1.78 and 1.11 mg C L^{-1}, respectively. Lower and upper 95% confidence intervals were 1.97 and 1.47 mg L^{-1} for May and 0.91 and 1.24 mg L^{-1} for November. Dawson et al. (2002) generally found concentrations <2 mg L^{-1} for free CO_2 in streams in peat dominated catchments in Scotland and Wales, although concentrations increased in areas of greater and thicker peat coverage, where gas retention in water may be higher and streams are more strongly coupled to the terrestrial environment and the super-saturated soil pore waters therein.

The initial regression model identifying catchment controls on free CO_2 gave a negative coefficient for altitude and a positive coefficient for neutral grassland. These variables suggest that greater concentrations of free CO_2 were found in low altitude catchments. However, the percentage of free CO_2 as a fraction of DIC in the low altitude catchments is the lowest in our survey (2–3%), and it may be that free CO_2 is highest in these catchments simply because DIC is highest. These catchments also have the highest water pH. Along with temperatures, these may influence the DIC speciation, and are accounted for in the calculation by ThinCarb of $EpCO2$. However, when macro-nutrients (TN, TP, DOC) were used to model free CO_2 concentrations, an improved model was found (Table 3). Thus, the concentration of free CO_2 in the river waters at the river/estuary interface appears to reflect the macro-nutrient status of the whole catchment, which in term suggests a relationship with land-use intensity. However, in the regression model, arable agriculture, population and urban area were not identified as explanatory variables. This may reflect the fact that some large urban areas (or large parts of them) are below the tidal limit (e.g. London), but also that greater population and land use intensity are found at lower altitudes, and are accounted for within this variable. The lack of relationship with arable land extent may simply reflect the dominance of grassland agriculture at a GB scale, which may therefore exert the greatest influence on river macronutrient concentrations. There appeared to be little effect of free CO_2 derived from groundwater sources (Pitman, 1978; Worrall and Lancaster, 2005). This is likely a reflection of the dominance of proximal sources of CO_2 in the lower river reaches, and the distal sources of CO_2 from groundwater higher up in the catchments. Subsequent calcite

precipitation, in addition to CO_2 degassing with travel from the source, may reduce free CO_2 concentrations from groundwater sources (e.g. Neal et al., 2002).

Increased soil respiration bought on by agricultural fertilisation (Borges et al., 2018) in the catchment has been identified in river waters. Over prolonged periods, regional increases in stream CO_2 evasion are positively correlated with total precipitation, with increased flushing from the soil a contributory factor (Butman and Raymond, 2011; Dawson et al., 2002). In addition, nutrients released from sewage effluent will contribute to in-stream production of free CO_2 (Marescaux et al., 2018; Wang et al., 2017). However, an additional groundwater influence may exist through the release of nutrients (particularly nitrate) from those rivers with a high base flow index (BFI) (Wang et al., 2013a, 2013b). Further evidence as to the role of nutrients in the concentrations of free CO_2 are the strong relationships between TN and TP (and PO_4-P and NO_3-N) with both altitude and annual average precipitation (SI:13 and SI:14). These relationships suggest that nutrient enrichment, and resulting higher rates of microbial respiration in the more intensive agricultural lowland catchments, are a driver of free CO_2 concentrations. These catchments have high population density and large nutrient load contributions from sewage effluent (Ascott et al., 2016; Jarvie et al., 2018; Holden et al., 2017; Bowes et al., 2011).

4.5. The flux and yield of free CO_2

The flux to estuaries (and potentially to the atmosphere) of CO_2 in 2017 was ~47.6 kt for the 39 rivers where estimates could be quantified (Fig. 4c). The only other available figure was a modelled estimate (Rawlins et al., 2014) based on the alkalinity of headwater streams analysed through the national geochemical sampling program (G-BASE) (Johnson et al., 2005). The Rawlins et al. (2014) study produced an estimate of CO_2 loss from England and Wales (68% of GB landmass) of 65.4 kt with 95% confidence limit of 46.1–77.2 kt. The figures of uncertainty quoted are associated with the prediction of pCO_2 concentrations and do not account for the uncertainties in the computation of flow or with stream temperature estimation (used to compute Henry's constant). These would also be of relevance in this study. Both the current and Rawlins et al. (2014) estimates should be considered high, as both assume complete CO_2 evasion. Indeed, the higher pH in coastal waters where CO_2 evasion is likely to occur would change the carbonate speciation such that free CO_2 is converted to HCO_3^- (free CO_2 in seawater is typically <0.5% of DIC). Nevertheless, this flux is likely to contribute to substantial CO_2 evasion as measured in GB estuarine waters (Yang et al., 2019). Whilst the Rawlins et al. (2014) estimate covers a larger area, it does not include the significant losses of CO_2 from the peatlands of Scotland, which are only partially accounted for in the estimates from our study.

For free CO_2 (Fig. 5c), there was a strong pattern of increased yield (t km^2 yr^{-1}) from catchments on the western side of GB, likely influenced by high average annual precipitation and thus runoff. In addition, the lower pH values of the rivers would ensure that free CO_2 would represent a higher proportion of the lower DIC concentrations. The chalk-based catchments of southern England had lower yields of free CO_2, possibly reflecting both higher water pH favouring HCO_3^-, longer residence times allowing degassing of groundwater derived $EpCO_2$, as well as lower precipitation. The lower yields may also partly reflect the effects of groundwater recharge on river flows in these lowland permeable catchments. Estimates of free CO_2 export from catchments in this paper are based on samples collected close to the tidal maximum, before entering the estuarine system. Therefore, this probably only represents a proportion of CO_2 that has evaded from catchments. Losses of catchment CO_2 through evasion can be greater than that carried as dissolved gas downstream (Billett and Moore, 2008). Other sources of catchment CO_2 evasion include surface waters such as ponds, lakes and reservoirs (Tranvik et al., 2009), peat and bog ecosystems, along with the head waters and tributaries of the major rivers. Estimates of CO_2 evasion from

catchment surface waters have been placed at ~10% (Sun et al., 2011) and ~ 70% (Hope et al., 2001) of net ecosystem exchange at the continental scale and peatland catchment scale, respectively. Headwater streams in particular have been identified as CO_2 sources within catchments with evasion being driven by turbulence generated by steep slopes, rough channel bottoms and high velocity (Maurice et al., 2017). Our river-estuary free-CO_2 yields may therefore represent only a small fraction of the CO_2 evasion that occurs within the catchment, with much degassed to the atmosphere upstream of the sampling points.

The model predicting free-CO_2 yield (t km^{-2} yr^{-1}) had coefficients which were negative for both arable and BFI suggesting that the larger intensive agricultural catchments and chalk-based ones (with High BFI and lower proportion of DIC as free CO_2) had a lower potential CO_2 evasion per km^2. This likely reflects their lower annual average precipitation and the greater recharge to aquifers, as they had relatively high concentrations of CO_2. This also suggests that groundwater does not act as a large source of EpCO2 at the tidal limit in the chalk and limestone dominated catchments because of the greater residence time of the water in rivers. Based on the total area of land our survey covered and the total flux (47.6 kt), a yield of 0.56 t C km^{-2} yr^{-1} can be derived which is slightly higher than the 0.44 t C km^{-2} yr^{-1} figure that Rawlins et al. (2014) published for England and Wales. For two peat dominated streams in Scotland, Dawson et al. (2002) reported yields of 0.26 and 0.87 t C km^{-2}.

There remains uncertainty in global estimates of CO_2 flux from riverine and freshwater systems to the atmosphere, with values estimated to be up to 4 Gt C yr^{-1} (Drake et al., 2017). Regardless, the figure obtained from the current study suggests a considerable export from terrestrial to estuarine systems where CO_2 evasion may occur (Laruelle et al., 2017). Examining ocean-air fluxes of CO_2 on the NW European shelf, Kitidis et al. (2019) suggest that most river-borne C losses largely occur within estuaries, with CO_2 accounting for much of this C loss. Whilst estuarine CO_2 efflux is biased towards large estuaries as these are where work is often focused, these large estuaries are also likely to be more urbanised/industrial, and have longer residence times for CO_2 efflux to occur.

4.6. Potential responses to environmental change

The current DIC concentration results are very similar to ones taken from a > 30 year dataset (SI:9). However, the flux of DIC from terrestrial ecosystems to the ocean may become more variable in the future, with land use and climate (temperature and precipitation) change potentially acting as drivers (Ren et al., 2015). Raymond and Hamilton (2018) acknowledge the difficulties in assessing chemical weathering because of the numerous interacting biotic and abiotic processes that have to be considered in assessing landscape level controls, even before the added complications of anthropogenic disturbances. However, future UK climate projections of increased probabilities of higher rainfall and temperature (Met Office, 2019) may introduce greater seasonal and spatial variability into the DIC cycle, possibly due to changes in chemical weathering rates and runoff (White & Blum, 1995; Oliva et al., 2003; Dessert et al., 2003). Temperature is less likely to induce major changes in DIC concentrations in the carbonate geology (chalk, limestone) of GB. It is recognised that soil pCO2 can be controlled by temperature and soil moisture which help determine ecosystem respiration (Romero-Mujalli et al., 2019) and it would be expected that higher pCO$_2$ concentrations would increase chemical weathering. However, in a global river study of rivers in carbonate rock-based catchments, a temperature effect was identified whereby river alkalinity concentrations appear to reach a maximum, before declining, at land temperatures ~11 °C (Gaillardet et al., 2019). This was primarily due to the role temperature plays on solubility in the carbonate system. Whilst, increased temperatures may increase pCO$_2$ through respiration, cold water would be expected to contain greater CO_2 leading to calcite dissolution being favoured at lower temperatures. Thus, the temperature effect on carbonate

dissolution intensity represents a balance of two competing mechanisms; the effect of increasing temperature on the thermodynamic constants of the carbonate system, particularly in decreasing Henry's constant countered by the increase in production of ecosystem soil CO_2 (Gaillardet et al., 2019). Other processes that may impact changes in DIC may involve the precipitation of secondary carbonates. Higher temperatures will increase soil respiration leading to increased pCO2 and during carbonate dissolution the water will equilibrate with the higher pCO$_2$ in soils. When the water comes into contact with air, degassing of CO_2 will increase the pH, promoting carbonate precipitation (Gaillardet et al., 2019). On the other hand, Ca and Mg silicate weathering may be expected to increase with temperature, without the same mineral precipitation constraints as those found for carbonate-based rocks, and unlike carbonates this weathering will be effective at drawing down CO_2 (Gaillardet et al., 1999).

However, changes are most likely to occur in runoff due to changes in seasonal precipitation and this may alter seasonal flux and yield. Results from this study have demonstrated the effect of relatively greater precipitation and runoff on DIC fluxes across the country. To add to the complexity of the DIC system, increasing temperature may increase soil respiration and also influence evapotranspiration rates, leading to changes in runoff and silicate weathering (Kelly et al., 1998; Richter and Billings, 2015).

Land-use change may also influence the future DIC budget. In agriculture, the expected trend is that there may be an increase in the area of arable farmland, with a decrease in grassland and continued reforestation and urban area expansion (CCC, 2020). To demonstrate the influence that different vegetation types have on DIC export, Kindler et al. (2011) examined losses of biogenically-derived DIC from grasslands, forests and croplands across Europe. They found leaching of biogenic DIC to be 8.3 ±4.9 g m^{-2} yr^{-1} for forests, 24.1+/− 7.2 g m^{-2} yr^{-1} for grassland and 4.1±1.3 g m^{-2} yr^{-1} for crop systems. This would suggest that any shift towards either arable and forest land coverage may alter DIC export. Concentrations of CO_2 have been found to be significantly higher in grasslands than forests because of the greater rates of root and microbial respiration, and because greater soil wetness reduces diffusion rates (Parfitt et al., 1997). In addition, if fertilised, there is the potential for increases in soil respiration, strong acid production (through nitrification) and weathering (Raymond and Hamilton, 2018).

Urbanisation within catchments may also impact DIC budgets through increasing sewage effluent discharges and urban diffuse runoff from impermeable surfaces (Barnes and Raymond, 2009). Differentiating the role of land-use in DIC loss to surface waters can be difficult to decouple from lithology and surficial materials, but some studies have found a possible response to urban areas. For example, Barnes and Raymond (2009) demonstrated that both agricultural and urban areas can enhance stream water DIC concentrations relative to forestry in a series of small catchments on the same bedrock and superficial geology. Those catchments with greater percentages of urban areas had higher DIC exports. This confirms other studies demonstrating increases in DIC observed in urban areas (Baker et al., 2008; Jarvie et al., 2017). Sources of DIC within urban systems may include weathering of $CaCO_3$ in concrete and the weathering of limestone road capping (Baker et al., 2008; Raymond and Hamilton, 2018). However, in our study the role of urban areas within catchments did not significantly improve model performance, possibly because there were strong links to altitude, since major urban areas are located in the lowland catchments.

Finally, increasing attention is being given to enhanced rock weathering (i.e. application of basaltic rock to agricultural land) as a means of removing CO_2 from the atmosphere (Beerling et al., 2020). This has been estimated to have a maximum technical potential for the UK of 19 Mt. CO_2 yr^{-1} to greenhouse gas removal in the UK (Simon et al., 2021). While large-scale implementation of enhanced weathering as a climate mitigation measure is unlikely in the near-term, even modest implementation could lead to measurable changes in the GB DIC flux. The application of agricultural liming has previously been identified in

DIC fluxes (Oh and Raymond, 2006). Potential exists for increased HCO_3^- flux to rivers and the increased precipitation of Ca, Mg and Fe carbonates in soils. In this context, our data provides an update on current DIC flux, and a valuable baseline against which to monitor and verify any additional CO_2 drawdown resulting from this process, and to support the assessment of any biogeochemical or ecological impacts.

5. Conclusions

Results from a year-long survey of 41 rivers across GB, representing 36% of the landmass and where land-cover was representative of the whole of Great Britain are reported. DIC represented ~69% of the total dissolved carbon flux from the surveyed catchments. The concentration, flux and yield recorded for DIC species supported previous published GB estimates, based on data collected between 10 and 30 years old. The study suggests that river DIC and HCO_3^- concentrations are largely controlled by catchment geology, whilst average annual precipitation influenced flux and yield. An average DIC yield of 8 13 t ha^{-1} yr^{-1} was calculated from the survey results. Concentrations of dissolved free CO_2 appeared to be related to catchment macro-nutrient status with probable sources being both from agriculture and urban land-uses (sewage treatment). Understanding this pool of dissolved CO_2 is of importance as it is a source of greenhouse gas emission through evasion to the atmosphere. Whilst increases in free CO_2 concentrations were linked to the lowland agricultural and densely populated catchments, yield estimates (t C Km^{-2} yr^{-1}) identified the northern, peat dominated catchments as being of great importance. An overall yield of 0.56 t C Km^{-2} yr^{-1} of free CO_2 was found for the sampled catchments. The results provide further evidence of the importance of land–ocean C fluxes in the national C budget, and offers an updated baseline for DIC land-ocean transport in GB.

Author contributions

Funding acquisition: Richard Sanders, Chris D. Evans, Vassilis Kitidis, Barry Rawlins, Dan J. Lapworth, Andrew P. Rees, Bryan M. Spears, Andrew Tye, Philip D. Nightingale, Daniel J. Mayor.

Conceptualization: Richard Sanders, Chris D. Evans, Vassilis Kitidis, Dan J. Lapworth, Andrew P. Rees, Bryan M. Spears, Andrew Tye, Philip D. Nightingale, Daniel J. Mayor, Nancy Dise.

Investigation: Andrew Tye, Jennifer L. Williamson, Helen P. Jarvie, Nancy B. Dise, Dan J. Lapworth, Don Monteith, Richard Sanders, Daniel J Mayor, Michael J. Bowes, Michael Bowes, Annette Burden, Nathan Callaghan, Gareth Farr, Stacey L. Felgate, Stuart Gibb, Pete J. Gilbert, Geoff Hargreaves, Patrick Keenan, Vassilis Kitidis, Monika D. Jürgens, Adrian Martin, Ian Mounteney, Philip D. Nightingale, M. Glória Pereira, Justyna Olszewska, Amy Pickard, Andrew P. Rees, Bryan Spears, Mark Stinchcombe, Debbie White, Peter Williams, Chris Evans.

Methodology: Richard Sanders, Chris D. Evans, Vassilis Kitidis, Dan J. Lapworth, Andrew P. Rees, Bryan M. Spears, Andrew Tye, Philip D. Nightingale, Mark Stinchcombe, Daniel J. Mayor.

Lab Analysis: Jenny Williamson, Patrick Keenan, M. Glória Pereira.

Formal analysis: Andrew Tye, Helen Jarvie.

Writing – original draft: Andrew Tye.

Writing – review & editing: Helen Jarvie, Richard Sanders, Chris D. Evans, Fred Worrall, Vassilis Kitidis, Don Monteith, Dan J. Lapworth, Andrew P. Rees, Bryan M. Spears, Andrew Tye, Jennifer L. Williamson, Mike Best, Stacey L. Felgate, Amy Pickard, Daniel J. Mayor, Nancy Dise.

Data curation: Andrew Tye, Adrian Martin.

Project Administration: Richard Sanders, Chris D. Evans, Daniel J. Mayor.

Data availability

Data is available through the Environmental Information Data Centre.

Declaration of Competing Interest

The authors declare that they have no known competing financial interests or personal relationships that could have appeared to influence the work reported in this paper.

Data availability

Data will be made available on request.

Acknowledgements

Appendix A. Supplementary data

Supplementary data to this article can be found online at https://doi.org/10.1016/j.jhydrol.2022.128677.

References

Amiotte-Suchet, P., Aubert, D., Probst, J.L., Gauthier-Lafaye, F., Probst, A., Andreux, F., Viville, D., 1999. δ13C pattern of dissolved inorganic carbon in a small granitic catchment: the Strengbach case study (Vosges mountains, France). Chem. Geol. 159, 129–145.

Ascott, M.J., Gooddy, D.C., Lapworth, D.J., Stuart, M.E., 2016. Estimating the leakage contribution of phosphate dosed drinking water to environmental phosphorus pollution at the national-scale. Sci. Total Environ. 572, 1534–1542.

Aufdenkampe, A.K., Mayorga, E., Raymond, P.A., Melack, J.M., Doney, S.C., Alin, S.R., Aalto, R.E., Yoo, K., 2011. Riverine coupling of biogeochemical cycles between land, oceans, and atmosphere. Front. Ecol. Environ. 9 (1), 53–60.

Baker, A., Cumberland, S., Hudson, N., 2008. Dissolved and total organic and inorganic carbon in some British rivers. Area 40 (1), 117–127.

Barnes, R.T., Raymond, P.A., 2009. The contribution of agricultural and urban activities to inorganic carbon fluxes within temperate watersheds. Chem. Geol. 266, 318–327.

Beerling, D.J., Kantzas, E.P., Lomas, M.R., et al., 2020. Potential for large-scale CO_2 removal via enhanced rock weathering with croplands. Nature 583, 242–248. https://doi.org/10.1038/s41586-020-2448-9.

Bell, V.A., Naden, P.S., Tipping, E., Davies, H.N., Carnell, E., Davies, J.A.C., Dore, A.J., Dragosits, U., Lapworth, D.J., Muhammed, S.E., Quinton, J.N., Stuart, M., Tomlinson, S., Wang, L., Whitmore, A.P., Wu, L., 2021. Long term simulations of macronutrients (C, N and P) in UK freshwaters. Sci. Total Environ. 776, 145813.

Billett, M.F., Harvey, F.H., 2013. Measurements of CO_2 and CH_4 evasion from UK peatland headwater streams. Biogeochemistry 114, 165–181.

Borges, A.V., Darchambeau, F., Lambert, T., Bouillon, S., Morana, C., Brouyère, S., Haloun, V., Jurado, A., Tseng, H.-C., Descy, J.-P., Roland, F.A.E., 2018. Effects of agricultural land use on fluvial carbon dioxide, methane and nitrous oxide

concentrations in a large European river, the Meuse (Belgium). Sci. Total Environ. 610-611, 342–355.

Bowes, M.J., Smith, J.T., Neal, C., Leach, D.V., Scarlett, P.M., Wickham, H.D., Harman, S. A., Armstrong, L.K., Davy-Bowker, J., Haft, M., Davies, C.E., 2011. Changes in water quality of the river Frome (UK) from 1965 to 2009: is phosphorus mitigation finally working? Sci. Total Environ. 409 (18), 3418–3430.

Butman, D., Raymond, P.A., 2011. Significant efflux of carbon dioxide from streams and rivers in the United States. Nat. Geosci. 4, 839–842.

Chaplot, V., Mutema, M., 2021. Sources and main controls of dissolved organic and inorganic carbon in river basins: a worldwide meta-analysis. J. Hydrol. 603, 126941.

Ciais, P., Sabine, C., Bala, G., Bopp, L., Brovkin, V., Canadell, J., Chhabra, A., DeFries, R., Galloway, J., Heimann, M., Jones, C., Le Quéré, C., Myneni, R.B., Piao, S., Thornton, P., 2014. Carbon and other biogeochemical cycles. In: Qin, D., Plattner, G. K., Tignor, M., Allen, S.K., Boschung, J., Nauels, A., Xia, Y., Bex, V., Midgley, P.M. (Eds.), Climate Change 2013: The Physical Science Basis. Contribution of Working Group I to the Fifth Assessment Report of the Intergovernmental Panel on Climate Change [Stocker TF]. Cambridge University Press, Cambridge, United Kingdom and New York, NY, USA.

Climate Change Committee, 2020. The Sixth Carbon Budget: The UK's path to net zero.

Dawson, J.J.C., Billett, M.F., Neal, C., Hill, S., 2002. A comparison of particulate, dissolved, and gaseous carbon in two contrasting upland streams in the UK. J. Hydrol. 257, 226–246.

Drake, T.W., Raymond, P.A., Spencer, R.G.M., 2017. Terrestrial carbon inputs to inland waters: a current synthesis of estimates and uncertainty. Limnol. Oceanogr. Lett. 3, 132–142.

Drake, T.W., Podgorski, D.C., Dinga, B., Chanton, J.P., Six, J., Spencer, R.G.M., 2020. Land-use controls on carbon biogeochemistry in lowland streams of the Congo Basin. Glob. Chang. Biol. 26, 1374–1389.

Dupré, B., Dessert, C., Oliva, P., Goddéris, Y., Viers, J., François, L., Millot, R., Gaillardet, J., 2003. Rivers, chemical weathering and Earth's climate. C.R. Geoscience 335, 1141–1160.

Graeber, D., Tenzin, Y., Stutter, M., Weigelhofer, G., Shatwell, T., von Tümpling, W., Tittel, J., Wachholz, A., Borchardt, D., 2021. Bioavailable DOC: reactive nutrient ratios control heterotrophic nutrient assimilation—an experimental proof of the macronutrient-access hypothesis. Biogeochemistry 155, 1–20.

Harley, J.F., Carvalho, L., Dudley, B., Heal, K.V., Rees, R.M., Skiba, U., 2015. Spatial and seasonal fluxes of the greenhouse gases N_2O, CO_2 and CH_4 in a UK macrotidal estuary. Estuar. Coast. Shelf Sci. 153, 62–73.

Holden, J., Haygarth, P.M., Dunn, N., Harris, J., Harris, R.C., Humble, A., Jenkins, A., MacDonald, J., McGonigle, D.F., Meacham, T., Orr, H.G., Pearson, P.L., Ross, M., Sapiets, A., Benton, T., 2017. Water quality and UK agriculture: challenges and opportunities. Wiley Interdiscip. Rev. Water 4, e1201.

Hope, D., Palmer, S.M., Billett, M.F., Dawson, J.J.C., 2001. Carbon dioxide and methane evasion from a temperate peatland stream. Limnol. Oceanogr. 46, 847–857.

Hunt, C.W., Salisbury, J.E., Bandemark, D., 2014. CO_2 input dynamics and air-sea exchange in a large New England estuary. Estuar. Coasts 37, 1078–1091.

Jarvie, H.P., Neal, C., Leach, D.V., Ryland, G.P., House, W.A., Robson, A.J., 1997. Major ion concentrations and the inorganic carbon chemistry of the Humber rivers. Sci. Total Environ. 194, 285–302.

Jarvie, H.P., Neal, C., Williams, R.J., 2004. Assessing changes in phosphorus concentrations in relation to in-stream plant ecology in lowland permeable catchments: bringing ecosystem functioning into water quality monitoring. Water Air Soil Pollut. 4, 641–655.

Jarvie, H.P., King, S.M., Neal, C., 2017. Inorganic carbon dominates total dissolved carbon concentrations and fluxes in British rivers. Application of the THINCARB model- thermodynamic modelling of inorganic carbon in freshwaters. Sci. Total Environ. 575, 496–512.

Jarvie, H.P., Smith, D.R., Norton, L.R., Edwards, F.K., Bowes, M.J., King, S.M., et al., 2018. Phosphorus and nitrogen limitation and impairment of headwater streams relative to rivers in Great Britain: a national perspective on eutrophication. Sci. Total Environ. 621, 849–862.

Johnson, C., Breward, N., Ander, E.L., Ault, L., 2005. G-BASE: baseline geochemical mapping of Great Britain and Northern Ireland. Geochem. 5, 1–13.

Kelland, M.E., Wade, P.W., Lewis, A.L., Taylor, L.L., Sarkar, B., Andrews, M.G., Lomas, M.R., Cotton, T.E.A., Kemp, S.J., James, R.H., Pearce, C.R., Hartley, S.E., Hodson, M.E., Leake, J.R., Banwart, S.A., Beerling, D.J., 2020. Increased yield and CO_2 sequestration potential with the C_4 cereal sorghum bicolor cultivated in basaltic rock dust-amended agricultural soil. Glob. Chang. Biol. 26, 3658–3676.

Kelly, E.F., Chadwick, O.A., Hilinski, T.E., 1998. The effect of plants on mineral weathering. Biogeochemistry 42, 21–53.

Kindler, R., Siemens, J., Kaiser, K., et al., 2011. Dissolved carbon leaching from soil is a crucial component of the net ecosystem carbon balance. Glob. Chang. Biol. 17, 1167–1185.

Kitidis, V., et al., 2019. Winter weather controls influx of atmospheric CO_2 on the north-west European shelf. Sci. Rep. 9, 20153.

Laruelle, G.G., Goossens, N., Arndt, S., Cai, W.-J., Regnier, P., 2017. Air–water CO_2 evasion from US East Coast estuaries. Biogeosciences 14, 2441–2468.

Li, M., Peng, C., Wang, M., Xue, W., Zhang, K., Wang, K., Shi, G., Zhu, Q., 2017. The carbon flux of global rivers: a re-evaluation of amount and spatial patterns. Ecol. Indic. 80, 40–51.

Marescaux, A., Thieu, V., Borges, A.V., Garnier, J., 2018. Seasonal and spatial variability of the partial pressure of carbon dioxide in the human-impacted Seine River in France. Sci. Rep. 8, 13961.

Maurice, L., Rawlins, B.G., Farr, G., Bell, R., Gooddy, D.C., 2017. The influence of flow and bed slope on gas transfer in steep streams and their implications for evasion of CO_2. J. Geophys. Res. Biogeosci. 122, 2862–2875.

Met Office, 2019. UKCP18 Science Overview Executive Summary January 2019. Crown Copyright 2019.

Meybeck, M., 1993. Riverine transport of atmospheric carbon: sources, global typology and budget. In: Terrestrial Biospheric Carbon Fluxes Quantification of Sinks and Sources of CO_2, pp. 443–463.

Neal, C., Jarvie, H.P., Williams, R.J., Pinder, L.C.V., Collett, G.D., Neal, M., Bhardwaj, L., 2000. The water quality of the great Ouse. Sci. Total Environ. 251 (252), 423–440.

Neal, C., Jarvie, H.P., Williams, R.J., Neal, M., Wickham, H., Hill, L., 2002. Phosphorus-calcium carbonate relationships in a lowland chalk river impacted by sewage inputs and phosphorus remediation: an assessment of phosphorus self-cleansing mechanisms in natural waters. Sci. Total Environ. 282-283, 295–310.

Oh, N.-H., Raymond, P.A., 2006. Contribution of agricultural liming to riverine bicarbonate export and CO_2 sequestration in the Ohio river basin. Glob. Biogeochem. Cycles 20, GB3012.

Öquist, M.G., Wallin, M., Seibert, J., Bishop, K., Laudon, H., 2009. Dissolved inorganic carbon export across the soil/stream interface and its fate in a boreal headwater stream. Environ. Sci. Technol. 43, 7364–7369.

Parfitt, R., Percival, H., Dahlgren, R., et al., 1997. Soil and solution chemistry under pasture and radiata pine in New Zealand. Plant Soil 191, 279–290.

Rawlins, B.G., Palumbo-Roe, B., Gooddy, D.C., Worrall, F., Smith, H., 2014. A model of potential carbon dioxide flux from surface water across England and Wales using headwater stream survey data and landscape predictors. Biogeosciences 11 (7), 1911–1925.

Raymond, P.A., Hamilton, S.K., 2018. Anthropogenic influences on riverine fluxes of dissolved inorganic carbon to the oceans. Limnol. Oceanogr. Lett. 3, 143–155.

Raymond, P.A., Oh, N.-H., Turner, R.E., Broussard, W., 2008. Anthropogenically enhnaced fluxes of water and carbon from the Mississippi River. Nature 451 (7177), 449–452.

Raymond, P.A., Hartmann, J., Lauerwald, R., Sobek, S., McDonald, C., Hoover, M., Butman, D., Striegl, R., Mayorga, E., Humborg, C., Kortelainen, P., Dürr, H., Meybeck, M., Ciais, P., Guth, P., 2013. Global carbon dioxide emissions from inland waters. Nature 503, 355–359.

Regnier, P., Resplandy, L., Najjar, R.G., Cias, P., 2022. The land-to-ocean loops of the global carbon cycle. Nature 603, 401–410.

Ren, W., Tian, H., Tao, B., Yang, J., Pan, S., Cai, W.-J., Lohrenz, S.E., He, R., Hopkinson, C.S., 2015. Large increase in dissolved inorganic carbon flux from the Mississippi River to Gulf of Mexico due to climatic and anthropogenic changes over the 21st century. J. Geophys. Res. Biogeosci. 120, 724–736.

Richter, D., Billings, S.A., 2015. 'One physical System': Tansley's ecosystem as Earth's critical zone. New Phytol. 206 (3), 900–912.

Rowland, C.S., Morton, R.D., Carrasco, L., McShane, G., O'Neil, A.W., Wood, C.M., 2017a. Land Cover Map 2015 (1km Percentage Target Class, GB). NERC Environmental Information Data Centre.

Rowland, C.S., Morton, R.D., Carrasco, L., McShane, G., O'Neil, A.W., Wood, C.M., 2017b. Land Cover Map 2015 (Vector, GB). NERC Environmental Information Data Centre.

Simon, R., Mitchell, A., Evans, C., Whitaker, J., Thomson, A., Keith, A., 2021. Greenhouse Gas Removal Methods and their Potential UK Deployment a Report Published for the Department for Business, Energy and Industrial Strategy by Element Energy and the UK Centre for Ecology and Hydrology.

Stets, E.G., Kelly, V.J., Crawford, C.G., 2014. Long-term trends in acidification in large rivers of the conterminous US in relation to acidification, agriculture and hydrologic modification. Sci. Total Environ. 488-489, 280–289.

Stutter, M.J., Graeber, D., Evans, C.D., Wade, A.J., Withers, P.J.A., 2018. Balancing macronutrient stoichiometry to alleviate eutrophication. Sci. Total Environ. 634, 439–447.

Suchet, P.A., Probst, J.-L., Ludwig, W., 2003. Worldwide distribution of continental rock lithology: implications for the atmospheric/soil CO_2 uptake by continental weathering and alkalinity transport to the ocean. Glob. Biogeochem. Cycles 17, 1038.

Tranvik, L.J., Downing, J.A., et al., 2009. Lakes and reservoirs as regulators of carbon cycling and climate. Limnol. Oceanogr. 54, 2298–2314.

Tye, A., et al., 2020. Monthly sampling of riverine chemistry and organic matter for 41 rivers in Great Britain in 2017 as part of the LOCATE project. In: NERC Environmental Information Data Centre. https://doi.org/10.5285/08223cdd-5e01-43ad-840d-15ff81e58acf.

Wang, Z.A., Bienvenu, D.J., Mann, P.J., Hoering, K.A., Poulsen, J.R., Spencer, R.G.M., Holmes, R.M., 2013a. Inorganic carbon speciation and fluxes in the Congo River. Geophys. Res. Lett. 40, 511–516.

Wang, L., Butcher, A.S., Stuart, M.E., Gooddy, D.C., Bloomfield, J.P., 2013b. The nitrate time bomb: a numerical way to investigate nitrate storage and lag time in the unsaturated zone. Environ. Geochem. Health 35 (5), 667–681.

Wang, X., He, Y., Yuan, X., Chen, H., Peng, C., Zhu, Q., Yue, J., Ren, H., Deng, W., Liu, H., 2017. pCO_2 and CO_2 fluxes of the metropolitan river network in relation to the urbanization of Chongqing, China. J. Geophys. Res. 122, 470–486.

Williamson, J.L., Tye, A., Lapworth, D.J., et al., 2021. Landscape controls on riverine export of dissolved organic carbon from Great Britain. Biogeochemistry. https://doi.org/10.1007/s10533-021-00762-2.

Worrall, F., Lancaster, A., 2005. The release of CO_2 from river waters - the contribution of excess CO2 from groundwater. Biogeochemistry 76 (2), 299–317.

Worrall, F., Howden, N.J.K., Burt, T.P., 2013. Assessment of sample frequency bias and precision in fluvial flux calculations - an improved low bias estimation method. J. Hydrol. 503, 101–110.

Yang, M., Bell, T.G., Brown, I.J., Fishwick, J.R., Kitidis, V., Nightingale, P.D., Rees, A.P., Smyth, T.J., 2019. Insights from year-long measurements of air–water CH_4 and CO_2 exchange in a coastal environment. Biogeosciences 16, 961–978.

Berner, R.A., 1998. The carbon cycle and carbon dioxide over Phanerozoic time: the role of land plants. Phil. Trans. R. Soc. Lond. B 353, 75–82.

R Core Team, 2018. R: A Language and Environment for Statistical Computing. R Foundation for Statistical Computing, Vienna https://www.R-project.org.

Littlewood, I.G., Watts, C.D., Custance, J.M., 1998. Systematic application of United Kingdom river flow and quality databases for estimating annual river mass loads. Science of the Total Environment 210 (211), 21–40.

Ludwig, W., Amiotte-Suchet, P., Munhoven, G., Probst, J.-L., 1998. Atmospheric CO2 consumption by continental erosion: Present-day controls and implications for the Last Glacial Maximum, Global Planet. Change 16–17, 107–120.

Pitman, J.I., 1978. Carbonate chemistry of groundwater from chalk, Givendale, East Yorkshire. Geochimica et Cosmochimica Acta 42 (12), 1885–1897.

Billett, M.F., Moore, T.R., 2008. Super saturation and evasion of CO2 and CH4 in surface waters at Mer Bleue peatland, Canada. Hydrological Processes 22, 2044–2054.

Sun, G., Caldwell, P., Noormets, A., McNulty, S.G., Cohen, E., Moore Myers, J., Domec, J.-C., Treasure, E., Mu, Q., Xiao, J., John, R., Chen, J., 2011. Upscaling key ecosystem functions across the conterminous United States by a water-centric ecosystem model. J. Geophys. Res. 116, 1–16.

White, A.F., Blum, A.E., 1995. Effects of climate on chemical weathering in watersheds. Geochimica et Cosmochimica Acta 59, 1729–1747.

Oliva, P., Viers, J., Dupré, B., 2003. Chemical weathering in granitic environments. Chemical Geology 202, 225–256.

Dessert, C., Dupre, B., Gaillardet, J., François, L.M., Allègre, C.J., 2003. Basalt weathering laws and the impact of basalt weathering on the global carbon cycle. Chemical Geology 202, 257–273.

Romero-Mujalli, G., Hartmann, J., Börker, J., Gaillardet, J., Calmels, D., 2019. Ecosystem controlled soil-rock pCO2 and carbonate weathering – Constraints by temperature and soil water content. Chemical Geology 527, 118634.

Gaillardet, J., Calmels, D., Romero-Mujalli, G., Zakharova, E., Hartmann, J., 2019. Global climate control on carbonate weathering intensity. Chemical Geology 527, 118762.

Gaillardet, J., Dupré, B., Louvat, P., Allègre, C.J., 1999. Global silicate weathering and CO2 consumption rates deduced from the chemistry of large rivers. Chem. Geol. 159, 3–30.